Global against Divided Optimization for the Participation of an EV Aggregator in the Day-ahead Electricity Market. Part II: Numerical Analysis

R.J. Bessa* and M.A. Matos

INESC TEC - INESC Technology and Science (formerly INESC Porto) and FEUP - Faculty of Engineering, University of Porto, Portugal

Abstract

This paper presents numerical analysis of two alternative optimization approaches intended to support an EV aggregation agent in optimizing buying bids for the day-ahead electricity market. A study with market data from the Iberian electricity market is used for comparison and validation of the forecasting and optimization performance of the *global* and *divided* optimization approaches. The results show that evaluating the forecast quality separately from its impact in the optimization results is misleading, because a forecast with a low error might result in a higher cost than a forecast with higher error. Both bidding approaches were also compared with an *inflexible EV load* approach where the EV are not controlled by an aggregator and start charging when they plug-in. Results show that optimized bids allow a considerable cost reduction when compared to an *inflexible load* approach, and the computational performance of the algorithms satisfies the requirements for operational use by a future real EV aggregation agent.

Keywords: Electric vehicles; aggregator; electricity market; forecasting; optimization; operational management.

1. Introduction

Policy makers and researchers working in electrical mobility have conducted studies for assessing the impact of electric vehicles (EV) in power system operation and planning [1] and the possible business models for companies operating in this activity [2]. The figure of an EV aggregation agent (aggregator in abbreviated form) has been proposed as an intermediary between vehicle driver, the system operators of the transmission and distribution grid and the electricity market [1][3]. The aggregator is an electricity retailer that has direct control over the charging process of the EV in its portfolio of clients and is responsible first for purchasing electrical energy for these clients in the electricity market and then to

*Correspondence to: INESC TEC (formerly INESC Porto), Campus da FEUP, Rua Dr. Roberto Frias, 378, 4200 - 465 Porto Portugal. Telf: +351 22 209 4208. Fax: +351 22 209 4050. E-mail: rbessa@inescporto.pt

control the charging process to comply with the contracted quantities of electrical energy.

A number of optimization algorithms for supporting the aggregator activity in the short-term horizon (i.e. participation in day-ahead markets) have been presented [4]-[9]. Two alternative bidding approaches (*global* and *divided*) for minimizing the cost of purchasing electrical energy in the day-ahead market are described in a companion paper [10]. The *global* approach uses aggregated values of the EV variables and the optimization model determines the bids exclusively based on total values. The *divided* approach uses individual information from each EV. Moreover, an operational management algorithm is used for minimizing the deviation between market bids and consumed electrical energy for charging EV. The models take as inputs forecasts from market prices and EV variables.

This paper presents numerical analyses for a realistic case-study with synthetic time series of availability and consumed electrical energy from an EV fleet, generated using statistics from the traffic patterns in Portugal. The two optimization approaches are evaluated and compared, and an assessment of the EV variables forecast's quality and value (i.e. economic benefits) is also presented.

This paper is organized as follows: sections 2 describes the case-study; section 3 presents the forecast evaluation results for the market and EV variables; section 4 compares the costs of the *global*, *divided* and *inflexible load* bidding approaches; section 5 presents the conclusions.

2. Case-Study Description

This section presents the case-study used for comparing and evaluating the bidding approaches. The case-study is more representative as possible and uses real electricity market data. Only EV data is synthetic and tries to simulate a forthcoming situation.

2.1 EV Synthetic Time Series

For producing time series of the EV availability and consumption, the generation mechanism for synthetic EV charging time series described in [11] was used. The movement of a fleet with 3000 battery EV along one year was simulated using a discrete-time-space Markov chain at each time step of half-hour, in accordance with the common traffic patterns in the northern region of Portugal [12]. The statistical post-processing of these traffic patterns is described in [13]. Having the EV movements fully defined, their power requirements were computed.

Each EV was initially characterized in terms of battery capacity, energy consumption and battery state of charge (SOC) in the beginning of the simulation. These values were defined according to truncated Gaussian probability density functions. The mean, standard deviation, maximum and minimum values are

given in [11]. The initial battery SOC values were defined as a parameter in the simulation, while the other two variables were gathered from the information made available by 42 different EV manufacturers. The charger efficiency was assumed to be 90%.

A specific driver behavior was also assigned initially to each EV. The possible behaviors considered in this paper were obtained from a survey made within the framework of the MERGE project [14]. The results revealed that there are three major types of behavior regarding EV charging, as presented in **Table 1**.

Table 1: Three types of behavior regarding EV charging.

For the drivers who charge their EV only when it needs, it was defined that the battery SOC threshold for charging equal to 40%.

The simulation methodology assumes that, at every time interval, each EV can be in one of the following states: in movement, parked in a residential area, parked in a commercial area or parked in an industrial area. When the state is "in movement", the energy consumption and the respective reduction in the battery SOC are computed. At each time interval, the EV battery SOC is updated according to the energy spent travelling or according to the energy absorbed from the electrical network.

Three charging levels were considered for the simulation: EV "parked in a residential area" and "parked in an industrial area" charge at 3 kW (slow charging mode), EV "parked in a commercial area" charge at 12 kW (normal charging mode) and the charging power in fast charging stations is 40 kW (fast charging mode) [14]. When an EV is parked, the decision of whether or not plugging it in for charging is made taking into consideration its driver behavior (see **Table 1**) and its current SOC (only for type C drivers). This case-study only studies EV parked in residential area (slow charging mode).

The simulation methodology provides, for a one-year period with 30 minutes time intervals, the following time series: the periods where EV are plugged-in and available to charge, the EV power absorbed at each time interval (assuming that the EV starts charging when plugs-in), the EV battery SOC evolution and the EV travelled distances. These time series are used for training the forecasting algorithms (as historical data) and testing the optimization and forecasting algorithms.

2.2 Electricity Market

The case-study follows the data and rules of the day-ahead Iberian electrical energy market [15]. The market agents may present buy and sell hourly bids that cover all 24 hours of the next day (physical delivery period). The gate closure occurs at the 10^{th} hour. Two types of simple hourly bids are possible: a

price independent bid for all hours regardless of the price level, with only a price cap, or a price dependent hourly bid for all hours where a stepwise curve is submitted.

In general, the day-ahead session structure and rules do not change from market to market. Therefore, the *global* and *divided* algorithms can be directly applied to different electricity markets without significant changes.

The total cost, in addition to the cost of purchasing electrical energy in the electrical energy market, also includes costs associated to deviations from planned consumption. When the aggregator has surplus of electrical energy in the market bid it has to sell this extra electrical energy at a regulation price ($p_t^{surplus}$) in general below the day-ahead electrical energy price; if the situation is shortage of electrical energy, it has to pay a regulation price ($p_t^{shortage}$) in general above the day-ahead electrical energy price [16]. This corresponds to the following equation for the total cost:

$$Total\ Cost = \sum_t \left(E_t^{cons} \cdot p_t + \begin{cases} \left(p_t - p_t^{surplus}\right) \cdot \left(E_t^{bid} - E_t^{cons}\right), E_t^{bid} > E_t^{cons} \\ \left(p_t^{shortage} - p_t\right) \cdot \left(E_t^{cons} - E_t^{bid}\right), E_t^{bid} < E_t^{cons} \end{cases} \right) \quad (1)$$

where E_t^{bid} is the electrical energy purchased in the day-ahead electrical energy market for time interval *t*, p_t is the day-ahead electrical energy price, E_t^{cons} is the consumed electrical energy, $p_t^{surplus}$ is the regulation price for positive deviations and $p_t^{shortage}$ is the regulation price for negative deviations.

The second component of this equation is the surplus or shortage costs, where the price difference p_t-$p_t^{surplus}$ is the positive deviations price (π_t^+), and the difference $p_t^{shortage}$- p_t is the negative deviations price (π_t^-).

The regulation prices, in the Portuguese control area, are related with the tertiary reserve (or regulation reserve) prices.

The electricity market data of the case-study is from a three years period (2009-2011) and consists of: electrical energy price of the day-ahead market for Portugal (downloaded from [17]); price of upward and downward reserve for Portugal (downloaded from [18]); interconnection exchanges (imported electrical energy) between Portugal and Spain (downloaded from [19]); load and wind power forecast in the Iberian peninsula for the next day (downloaded from [17]).

In general, the European market designs have different penalization prices for negative and positive real-time deviations from the market dispatch [20]. These prices result from regulation market sessions (e.g. with manual reserve bids cleared in real-time by the system operator) or are established by the regulator to provide incentives for better resources' scheduling. The operational management algorithm

123 can be generalized for any electricity market with asymmetric or symmetric regulation prices. Other
124 market designs, such as the U.S. markets, have a real-time market session where the price difference for
125 the day-ahead market price can induce significant losses in case of deviation from the day-ahead bid [21].
126 In this case, the objective function of the operational management algorithms needs to be redesigned to
127 include this price difference, which, depending on the deviation sign, might represent a profit for the
128 aggregator (sell surplus of electrical energy at a higher price).

129 Finally, this paper does not consider the participation in intraday and hour-ahead markets [22],
130 although this is an important topic for future work. The participation in the intraday market sessions is
131 not mandatory, but it is foreseen that the aggregator will use these sessions to calculate new bids using
132 updated information (e.g. forecasts). For example, if the amount of forecasted consumption for the time
133 intervals covered by the intraday session is larger than the amount contracted in the day-ahead session (or
134 in the previous intraday session), the aggregator must buy the deficit of energy from the pool at the
135 intraday price (which represents a cost increase). Conversely, if the amount of forecasted consumption is
136 smaller than the amount contracted in the day-ahead session (or in the previous intraday session), the
137 aggregator makes an offer for selling this electrical energy surplus in the intraday market (obtaining profit
138 if the intraday market price is higher than the day-ahead price). In both cases, the aggregator is mitigating
139 deviation penalties.

140 ### 2.3 Participation in the Electricity Market

141 **Figure 1** depicts a diagram with the sequence of tasks from the aggregator participation in the Iberian
142 electricity market. Before the 10^{th} hour of day 0, the aggregator forecasts the market and EV variables,
143 computes optimal bids based on these forecasts, and then presents bids in the day-ahead electrical energy
144 market. The market settlement process takes place between the 11^{th} and 14^{th} hours of day 0. Then, during
145 the 24 hourly intervals of day 1, the aggregator manages the EV individual charging for minimizing the
146 deviation between bids (presented in day 0) and actual consumption.

Figure 1: Diagram with the sequence of tasks for participating in the Iberian electricity market.

147 **Figure 2** depicts the diagram with the temporal horizons of the forecast and optimization algorithms
148 for the Iberian electricity market. The bidding optimization is performed for the market settlement period
149 (24 hourly intervals in day 1), but extended to have 12 additional hours since most of the EV are expected
150 to depart in day 2. Since the gate closure of the day-ahead electrical energy market is the 10^{th} hour, the
151 aggregator needs to forecast the EV variables for a time horizon of 100 half-hour time intervals (i.e.

between the 10th of day 0 and the 12th hour of day 2). Only the forecast between the first time interval of day 1 and the 12th time interval of day 2 is an input of the bidding optimization model.

Figure 2: Diagram with the temporal horizons of the forecast and optimization algorithms.

The output of the bidding optimization until the 24th hour of day 1 is one input of the bidding optimization exercise in day 2 (as illustrated by the arrow in **Figure 2**), and this interaction is repeated in each day. This guarantees the temporal continuity of the charging process.

The output of the market settlement (accepted bids) is an input of the operational management algorithm. The time horizon of the algorithm is variable and equal to the maximum of departure hour of all the EV. The time step is the same of the *global* or *divided* approaches, which is half-hour. The output until the 24th hour of day 1 is an input of the subsequent optimization in day 2 (as illustrated by the arrow in **Figure 2**).

The two bidding approaches will be compared with the situation where all the clients are *inflexible EV loads*. In this mode, the EV driver is completely free to connect and charge the vehicle whenever he/she wants. The charging starts automatically when the EV plugs-in. The aggregator in this case is a standard electricity retailer that forecasts the total consumption and offers in the day-ahead electrical energy market a bid equal to the forecasted values for each time interval.

2.4 Sampling Process for Evaluation

For a robust evaluation of the bidding's results in section 4, a sampling process based on the evaluation made in [23] was adopted for producing random repetitions of a simulation experiment. The objective is to evaluate the optimization results for different market data randomly sampled (but maintaining the temporal sequence) from the three year period. Since the forecasting algorithms require training and testing datasets, a fixed length for these two sets was defined: 9 months for the training dataset, 3 months for the testing dataset.

Then, a sampling process without replacement is used to draw the first hour of the day, *t*, from the candidate set. This sample is used to split the three years of data in training (between t and t-9 months) and testing (between t and t+3 months) datasets. The process is repeated 100 times, and for each sample *t*, the *global* and *divided* optimization algorithms are applied to the test dataset, and corresponding costs of purchasing electricity are computed. The result, instead of a single value for the total cost, is a distribution with 100 samples.

This sampling process is only used in the electricity market data. Because of a high calculation time (in

particular in the *divided* approach), it is not possible to apply this process to the EV data. In order to test the optimization methodologies in different EV data, the synthetic time series for 3000 EV is divided in two groups of 1500 EV: datasets A and B. Moreover, each EV dataset is divided in training and testing periods: the first 9 months for training and the last 3 months for testing.

3. Evaluation of the Forecasting Performance

3.1 Aggregated EV Variables

Three different EV variables are required for the *global* approach: total maximum available power for charging, total charging requirement and charging requirement distribution. Moreover, for the *inflexible EV load* approach it is also necessary to forecast the total consumption.

The application of the unit-roots Kwiatkowski-Phillips-Schmidt-Shin (KPSS) test [24] showed that all the four time series are stationary. The analysis of the autocorrelation diagrams for the aggregated variables shows a daily (higher peak in lag 48) and weekly (higher peak in lag 336) patterns. Therefore, based on the autocorrelation diagram and using the Akaike information criterion (AIC)[25] as a performance metric, the following model was used for forecasting the four variables:

$$y_t = \phi_0 + \phi_1 \cdot y_{t-1} + \phi_2 \cdot y_{t-2} + \phi_3 \cdot y_{t-48} + \phi_4 \cdot y_{t-336} + H_t + D_t \quad (2)$$

where ϕ are the model's coefficients, y_{t-j} is the j[th] lag of the response variable y, l is the lag order, H_t is a seasonal index that takes a different value for each hour of the day, and D_t is a seasonal index that takes a different value for each day of the week.

The following metrics measure the forecast statistical quality. The classical MAPE (Mean Absolute Percentage Error), given by

$$MAPE = \frac{1}{N} \sum_{j=1}^{N} \left(\frac{|y_j - \hat{y}_j|}{y_j} \right) \cdot 100 \quad (3)$$

where y_j is the realized value, $\hat{y}_j$ the forecasted value and N the number of samples in the test dataset. The modified MAPE for time series with zero values [26]:

$$mMAPE = \frac{\sum_{j=1}^{N} \left(|y_j - \hat{y}_j| \right)}{\sum_{j=1}^{N} \left(y_j \right)} \cdot 100 \quad (4)$$

The percentage bias:

$$PBIAS = \frac{1}{N} \sum_{j=1}^{N} \left(\frac{\left(y_j - \hat{y}_j \right)}{y_j} \cdot \right) 100 \quad (5)$$

A modified percentage bias (mPBIAS) similar to Eq. 4 is used in variables with zero values.

Table 2 presents the forecasting quality evaluation for the four EV variables in dataset A and B. The

forecast time horizon is 100 look-ahead time steps (half-hour data). The error values show that the forecasts present a good quality.

Table 2: Forecasting performance for the EV aggregated variables for dataset A and B.

It is important to stress that these statistical performance metrics, in particular for the charging requirement variable, measure only the forecast quality (i.e. match between forecasted and realized value). In fact, their true forecast value can only be assessed by computing the total cost of the bidding process. For example, the forecasts could indicate a 16 kWh of charging requirement that need to be satisfied until hour 6h, while the realized value is 16 kWh until hour 8h. This represents a high forecast error in the mMAPE sense, but, actuality, it corresponds only to an anticipation of the charging requirement. An evaluation of the economic value will be presented in section 4.

3.2 Individual EV Variables

For each EV, the availability is first forecasted and then non-parametric bootstrapping is used to estimate the charging requirement for each plugged-in period.

The three different drivers' behavior of **Table 1** have availability time series with different autocorrelation diagrams. The difference is particularly clear between types A/B and type C. EV drivers of type A and B have a clear double seasonal pattern (i.e. daily and weekly), while type C drivers' behavior does not have a seasonal cycle. Because of different autocorrelation patterns, two Generalized Linear Models (GLM) were considered:

$$p(y_t = 1 \mid y_{t-1} \cdots y_{t-l}) = 1/(1 + \exp(-(\phi_0 + \phi_1 \cdot y_{t-1} + \phi_2 \cdot y_{t-2} + \phi_3 \cdot y_{t-3} + \phi_4 \cdot y_{t-48} + \phi_5 \cdot y_{t-336}))) \quad (6)$$

for type A and B drivers, and

$$p(y_t = 1 \mid y_{t-1} \cdots y_{t-l}) = 1/(1 + \exp(-(\phi_0 + \phi_1 \cdot y_{t-1} + \phi_2 \cdot y_{t-2} + \phi_3 \cdot y_{t-3} + \phi_4 \cdot y_{t-4}))) \quad (7)$$

for type C drivers. In both cases, y is a binary variable indicating whether or not the EV is plugged-in and $p(y_t=1|y_{t-1}\ldots y_{t-l})$ is the posterior probability.

The same lagged variables were used for all EV from the same type. A topic for future research is to develop an automatic procedure for selecting different input variables for each EV.

The performance of the availability forecast is measured with a metric from the literature about evaluation in classification problems [27]:

$$Accuracy = \sqrt{\frac{TP}{TP + FP} \cdot \frac{TP}{TP + FN}} \cdot 100 \quad (8)$$

where TP is the number of correct plugged-in predictions (true positives), FN is the number of wrong

zero predictions (false negative) and *FP* is the number of wrong plugged-in predictions (false positive).

Figure 3 summarizes the availability forecast results divided by drivers' type with a boxplot for the two datasets, and for a time horizon up to 100 time intervals ahead.

Figure 3: Boxplot for the accuracy of the availability forecast and for dataset A and B. The boxplot have five statistics: lowest datum (within 1.5 IQR) of the lower quartile, lower quartile, median, upper quartile, and the highest datum (within 1.5 IQR) of the upper quartile. The outliers are also identified on the boxplot.

The availability forecast for type C drivers presents the lowest accuracy, suggesting that these availability patterns are difficult to forecast. Some forecasts for type A drivers also present a very low accuracy. The forecasts with low accuracy for type A and C drivers have in common a low number of time intervals in one year during which the EV is plugged-in for charging. For example, an EV of type A with accuracy equal to 4.31% is only plugged-in during 24.60% of one year time, and a type C driver with accuracy equal to 4.76% is only plugged-in during 12.37%. EV with better performance has a higher rate of plugged-in hours. For example, an EV with 80% of accuracy is plugged-in during 52.5% of the time.

These results suggest that the asymmetry in the number of plugged-in hours has a considerable impact on the model performance.

The mMAPE computed for the aggregated availability (sum of the individual availability forecasts) is 6.99% for dataset A, and 8.09% for dataset B. The modified PBIAS is 4.45% in dataset A, and -4.60% for the dataset B. These results show a good forecast quality for the aggregated availability.

As mentioned in the previous section, the individual charging requirement forecast quality cannot be assessed with classical statistics that quantify the difference between realized and forecasted value. Nevertheless, the aggregated values of the individual forecasts can give a reference value for comparison with the values in **Table 2**. For dataset A the mMAPE is 29.93%, while for dataset B it is 30.69%. These errors are higher than the ones of the aggregated variables from the previous section, but only the evaluation of the final deviations' magnitude and cost can give a true picture of the forecast error.

3.3 Market Prices

The KPSS test showed that the price time series are non-stationary and a differentiation of order 1 is needed. Moreover, based on the autocorrelation diagram and using the AIC, the following model was used for forecasting the day-ahead electrical energy price:

$$\hat{p}_t = p_{t-1} + \phi_1 \cdot p_{t-1} + \phi_2 \cdot p_{t-2} + \phi_3 \cdot p_{t-3} + g(wp_t) + H_t + D_t \quad (9)$$

where p_{t-j} is the jth lag of the price variable, l is the lag order, H_t takes a different value for each hour

of the day, and D_t takes a different value for each day of the week, g are cubic basis splines, and wp is the forecasted wind power penetration.

The interior knots of the basis splines were placed in each quantile according to 6 degrees of freedom (which attains the lowest AIC). The boundary knots were placed in the extremes of the data.

For forecasting the negative deviation price (i.e. difference between shortage regulation and electrical energy price) the following model was used:

$$\hat{\pi}_t^- = \pi_{t-1}^- + \phi_1 \cdot \pi_{t-1}^- + \phi_2 \cdot \pi_{t-2}^- + \phi_3 \cdot \pi_{t-3}^- + g(wp_t) + g\left(I_t^{\text{Import}}\right) + g(p_t) + H_t + D_t \quad (10)$$

where p_t is the electrical energy price of the day-ahead market, I_t^{import} is the interconnection exchange (imported electrical energy) of the bulk power system that results from the market mechanism and wp_t is the forecasted wind power penetration. The degree of freedom for this model is 10.

For the positive deviation price $\pi^+{}_t$ (i.e. difference between surplus regulation and electrical energy price) the model of Eq. 11 is used, but with I_t^{Import} replaced by I_t^{Export}.

For participating in the market with buying bids, the most important information is the ranking of the prices [5]. Therefore, in addition to the mean absolute error (MAE), the Spearman rank correlation is used for measuring the prices ranking quality. The Spearman correlation coefficient is computed for each pair of forecasted and realized values of a time horizon of 36 hours ahead, and then averaged over the entire test period. **Figure 4** depicts boxplots summarizing the evaluation results in the 100 random samples for the three market variables: electrical energy, surplus and shortage prices.

Figure 4: Spearman correlation and mean absolute error of the prices forecasts for 100 samples.

The performance of the electrical energy price is acceptable, the median for the rank correlation is 0.77 and MAE is 5.21 €/MWh. The forecasts for the deviation prices present a low performance because their rank correlation is around 0.25 for both prices. The shortage price presents a low MAE (median of 7.45 €/MWh) when compared to the surplus price (median of 11.67 €/MWh). These results indicate that the forecasting approach for the deviations prices has room for improvement.

3.4 Computational Implementation Issues

The presented case-study was tested on a laptop computer with an Intel Core i5 CPU M450 @ 2.40 GHz processor and 4 GB of RAM memory.

In order to forecast the aggregated variables (Eq. 2), function *gls* from R package *nlme* [28] was used for fitting a linear model using generalized least squares. The execution time for estimating the model's parameters is 106 seconds on average. However, this task is conducted offline and only one time. The

average execution time was 0.45 seconds for producing a single forecast with 100 look-ahead time steps.

For fitting the price forecasting models (Eq. 9-10) the function *gam* from R package *mgcv* [29] was used. The average execution time for parameters' estimation was 0.78 seconds and 0.42 seconds for a single forecast with 36 look-ahead time steps.

For forecasting EV availability, the function *bayesglm* from R package *arm* [30] was used for fitting the GLM. The charging requirement was estimated with a bootstrapping process. The execution time for the charging requirement forecast (including the GLM training and availability forecast) was 8.56 seconds for one EV and for a single forecast with 100 look-ahead time steps. The execution times of this forecasting algorithm might be prohibitive if the number of EV is high. However, this process can be parallelized and an implementation in C or Fortran would increase considerably the computational performance. For the simulations, the execution time is of several hours when simulating thousands of EV for a test period with 3 months.

4. Comparison between Global and Divided Bidding Approaches

In this section, the sampling process described in section 2.4 is used for comparing the costs of the *global* and *divided* approaches for 100 samples. For the *global* approach, it is necessary to set the value of one parameter, β. This parameter is included in a constraint of the optimization problem where the purchased electrical energy is limited by the forecasted total maximum available power (P^{max}). P^{max} is adjusted, as the charging process evolves, linearly using β; more details can be found in [10]. The β value was estimated from the first 9 months (training dataset). For each β, the mMAPE was computed and the β value that leads to its lowest value was selected. The result was a β equal to 1.0 and 0.8 for datasets A and B.

4.1 Computational Implementation Issues

The optimization problems were solved with IBM ILOG CPLEX optimizer [31] using the Python API. For the global optimization, the number of decision variables is 72 (for a programming horizon of 72 half-hours time intervals), the number of constraints is 216, and the execution time on average was 0.041 seconds. For the divided optimization, the number of decision variables and constraints varies with the number of EV plugged-in in each time interval. For example, for the day 1 of the case-study, the number of decision variables was 43,461 and the number of constraints was 46,078. The average execution time was 0.639 seconds.

The number of decision variables and constraints in the operational management algorithm also varies

with the number of EV plugged-in in each time interval. For the first time interval of day 1 (period between 0 and 1 AM with 1096 plugged-in EV) the number of decision variables was 17,952 and the number of constraints was 19,079. The average execution time was 0.475 seconds.

4.2 Visual Comparison of Days

Figure 5 depicts a visual comparison between the two bidding approaches (i.e. optimized bids) for the 6^{th} day from the test dataset of a sample.

Figure 5: Optimized bids obtained from the *divided* and *global* approaches for the 6^{th} day of the test period.

The plots show dissimilarity between the two approaches in all the time intervals. The *global* approach has time intervals with no bids in both days (in particular during the last ten time intervals), while the *divided* approach has bids in all the time intervals. This suggests that the bids from the *global* approach are more concentrated, which may create difficulties in avoiding deviations. Conversely, the bids from the *divided* approach are more dispersed, which may facilitate the operational management algorithm. As expected, the hours with the highest bid values are during the night, where the forecasted prices have low values.

4.3 Comparison of the Deviations between Bid and Realized Consumption

The deviation between bid and realized consumption is measured by the mMAPE. **Figure 6** depicts boxplots for the *divided* approach with forecasted information and for both datasets. Since the EV dataset is always the same in each random sample, this variation in deviations from sample to sample is only because of different electrical energy and deviation prices. In other words, these deviations occur because the bids are placed in different time intervals according to the forecasted prices. The small variation in both metrics indicates that the *divided* approach is robust to the electricity market conditions (i.e. prices ranking).

Figure 6: mMAPE of the *divided* approach with forecasted information for dataset A and B.

Figure 7 depicts the mMAPE for the *global* approach with forecasted and realized values (of EV and market variables) as input. The deviations in this bidding approach, in contrast to the *divided* approach, have a more widespread variation for different market conditions. For example, the mMAPE boxplot for dataset A with forecasted information varies between 19% and 29%. Note that, as demonstrated in a companion paper [10], the global model with realized values presents deviations. These deviations are not due to forecast errors, but related to information loss when only aggregated values are used as input for computing the optimal bid.

Figure 7: mMAPE of the *global* approach with forecasted and realized information for dataset A and B.

4.4 Comparison of the Costs from Participating the Electricity Market

This section compares the costs from participating in the electricity market. **Figure 8** depicts the total cost (computed with Eq. 1) of the *divided* approach with perfect and forecasted information. In both datasets, the difference between the total cost obtained with perfect and forecasted information is low. The difference between the medians is 1.73 k€ (24.69-22.9 k€, cost increase of 7.5%) for dataset A and 3.15 k€ (57.77-54.62 k€, cost increase of 5.76%) for dataset B. This cost difference suggests that more advanced bidding models, including stochastic information, can only improve over this small percentage.

Figure 8: Results with perfect and forecasted information for the *divided* approach in dataset A and B.

Figure 9 depicts the total cost of the *global* approach with realized and forecasted values as input. The difference between medians is 0.62 k€ (26.60-25.98 k€, cost increase of 2.4%) for dataset A and 1.48% (64.18-62.70 k€, cost increase of 2.36%). These results indicate that the forecast errors have a low impact on results. This is an expected conclusion since, as shown in section 3, the forecast error for the aggregated variables is low. This low impact of forecast errors is traded-off with deviation costs originated from modeling the EV fleet only with aggregated information.

Figure 9: Results with perfect and forecasted information for the *global* approach in dataset A and B.

Figure 10 depicts the total cost and its three components: cost of electrical energy purchased in the day-ahead market ($E^{bid}.p$), cost of positive deviations or surplus cost ($\pi_t^+.[E^{bid}-E^{cons}]$ in Eq. 1), and cost of negative deviations or shortage cost ($\pi_t^-.[E^{cons}-E^{bid}]$ in Eq. 1). For comparison, the costs obtained with all EV as *inflexible loads* are also presented.

Figure 10: Costs comparison between *divided, global* and *inflexible EV load* approaches obtained using forecasted values for dataset A.

The *global* approach has the highest deviation costs since it also has the highest deviation values. Nevertheless, in all the approaches the deviation costs are marginal compared to the day-ahead cost. Since the two bidding approaches were underestimating the charging requirement, the shortage costs are higher on average compared to the surplus cost. The *inflexible load* approach has a low deviation value, but the surplus cost is higher than the *divided* approach.

The approach with the lowest day-ahead and total cost is the *divided* approach, followed by the *global* approach. The median of the total costs is 24.69 k€ for the *divided* approach, 26.60 k€ for the *global* and 31.29 k€ for the *inflexible load*. This translates to a 26.7% total cost decrease in the *divided* approach

compared to the *inflexible load*, and a 17.6% decrease in the *global* approach. Note that the main contribution to increase the total cost of the *inflexible load* is from the day-ahead cost, since the EV are charged in more expensive time intervals.

Figure 11 depicts the total cost and components for dataset B. The *divided* and *global* approaches have a lower difference between surplus and shortage costs, compared to dataset A. In this dataset, the ratio between deviation and day-ahead costs is lower, compared to dataset A.

Figure 11: Costs comparison between *divided*, *global* and *inflexible EV load* approaches obtained using forecasted values for dataset B.

The median of the total costs is 57.76 k€ for the *divided*, 64.17 k€ for the *global* and 68.34 k€ for the *inflexible load*. This translates to an 18.3% total cost decrease in the *divided* and 6.6% decrease in the *global* approach.

An academic exercise was conducted for finding *a posteriori* the retailing tariff that leads to a breakeven between total cost and retailing revenue for the three bidding approaches. The retailing revenue for different values of a fixed retailing tariff was computed by multiplying the consumed electrical energy by the tariff value. The tariffs associated to the use transmission and distribution networks were ignored because their values are independent from the bidding approach. The average retailing profit from the 100 samples is given by the average retailing revenue from applying a specific tariff minus the average total cost. The breakeven point is the tariff value that makes retailing profit positive.

Table 3 presents the tariff value that leads to breakeven between total cost and retailing revenue. The tariff values show that the aggregator with the *divided* approach can offer a reduction in the retailing tariff of around 36.4% in dataset A and around 20% in dataset B compared to the *inflexible* approach. With the *global* approach, the aggregator can offer a discount of around 25% in dataset A and around 10% in dataset B. With this cost reduction, the aggregator either keeps unchanged the retailing tariffs and obtains a profit increase or offers a reduction in the retailing tariffs for attracting new clients.

It is important to stress that these tariff values are theoretical and only indicative because the definition of a retailing tariff is much more complex and requires mid-term portfolio optimization [32]. Moreover, the tariff value varies also with the EV fleet behavior and characteristics.

Table 3: Retailing tariff value that leads to a breakeven between total cost and retailing revenue.

5. Conclusions

This paper presented the numerical results for the two alternative optimization and forecasting

approaches for an EV aggregator participating in the Iberian electricity market with two fleets of 1500 EV.

The forecasting results show that the algorithms provide acceptable quality to be used as input for optimizing the day-ahead bids. The error of the aggregated variables used in the *global* approach is low, and the evaluation of the total cost indicated that advanced forecasting algorithms can only accomplish improvements over a small percentage. The forecasts for the individual EV variables lead to a low deviation in the *divided* approach, which suggests an acceptable quality.

The results showed that the operational management algorithm is crucial for decreasing deviation costs by combining the EV individual charging. This was particularly significant in the *divided* approach where a forecast error of around 30% for charging requirement resulted in a final deviation of around 9.5%.

The comparison between *global*, *divided* and *inflexible load* bidding approaches lead to the following conclusions: i) the *global* approach has a higher deviation value compared to *divided* one, which results in a higher total cost. For instance, in one EV fleet the *divided* approach reduced the total cost around 11% compared to the *global* approach; ii) the *divided* approach is more robust to different EV fleets and electrical energy price patterns. For the two EV datasets and a sampling process with 100 samples, the deviation in the *divided* approach ranged from 8.5% to 12%, while in the *global* approach ranged from 18% to 30%; iii) the *inflexible load* approach also benefits from aggregating EV, which leads in low forecast error. However, the total cost is high because the EV are charged during high price periods; iv) a bidding optimizing model allows a discount in the retailing tariff of 20% and 36%, compared to an *inflexible load* approach, in two different EV fleets.

The algorithms presented a computational performance acceptable for practical applications.

As an overall conclusion, the results in this paper show that EV drivers under a contract with the aggregator have one important advantage: the aggregator supports the deviations costs, and combines the EV for decreasing the deviation costs.

Conversely, in a situation where the EV behaves as an independent and intelligent agent that could interface directly with the electricity market (not allowed by the current market rules for small loads), the driver must support financially its deviation costs. Nevertheless, it is probable that in this mode, the driver will use a route planning software for a better schedule of its trips and bids. In any case, this may result in high deviation from planning and consequently high deviation costs that must be supported by the driver.

The forecasting and optimization algorithms were tested with EV synthetic data anticipating a future

scenario. Nevertheless, the conclusions from this paper can be generalized to case-studies with real EV data and the algorithms can be applied without any change.

Future work consists in extending the operational management and forecasting algorithms to include the possibility of upward and downward reserve bids. Furthermore, there is also a potential for improvement in the forecasting algorithms for the *divided* approach.

Appendix – Sensitivity Analysis of the β Parameter

This annex presents a sensitivity analysis of the β parameter that was conducted for EV datasets A and B and the market data was from a period between October and December 2010.

Figure 12 depicts the total cost, day-ahead cost, shortage and surplus costs for the global approach with different values of β (ranging from 0 to 1 with 0.05 increments), and for dataset A.

The plot shows that the day-ahead cost increases with β. This means that a lower β gives more "freedom" to the optimization algorithm for placing the bids in the time intervals with the lowest price. Conversely, this "freedom" results in a deviations increase, and consequently in an increase of shortage and surplus costs. The addition of these three costs results in a total cost increase when β decreases.

Figure 13 depicts the same analysis for dataset B. The day-ahead cost decreases with β but the surplus and shortage costs start to increase when β is greater than 0.8.

Figure 12: The impact of *β* in the total cost shares for dataset A with 1500 EV.

Figure 13: The impact of *β* in the total cost shares for dataset B with 1500 EV.

Acknowledgements

This work was supported in part by Fundação para a Ciência e Tecnologia (FCT) under Grant SFRH/BD/33738/2009, and by the European Union within the framework of the European Project MERGE-Mobile Energy Resources in Grids of Electricity, Contract 241399 (7th Framework Programme).

The authors acknowledge Filipe J. Soares from INESC TEC for providing the electric vehicles synthetic time series data used in this paper. The market data and EV synthetic time series can be made available upon request.

References

[1] J.A. Peças Lopes, F.J. Soares, P.R.R. Almeida, Integration of electric vehicles in the electric power system, Proc. of the IEEE 99 (2011) 168-183.

[2] F. Kley, C. Lerch, D. Dallinger, New business models for electric cars - a holistic approach, Energy Policy 39 (2011) 3392-3403.

[3] C. Guille, G. Gross, A conceptual framework for the vehicle-to-grid (V2G) implementation, Energy Policy 37 (2009) 4379-4390.

[4] R.J. Bessa, M.A. Matos, F.J Soares, J.A. Peças Lopes, Optimized bidding of a EV aggregation agent in the electricity market, IEEE Trans. on Smart Grid 3 (2012) 443-452.

[5] D. Wu, D.C. Aliprantis, L. Ying, Load scheduling and dispatch for aggregators of plug-in electric vehicles, IEEE Trans. on Smart Grid 3 (2012) 368-376.

[6] T.K. Kristoffersen, K. Capion, P. Meibom, Optimal charging of electric drive vehicles in a market environment, Appl. Energy 88 (2011) 1940-1948.

[7] O. Sundstrom, C. Binding, Planning electric-drive vehicle charging under constrained grid conditions, Proc. of the 2010 Inter Conf. on Power Sys. Tech. (2010), Hangzhou, China.

[8] E. Sortomme, M.A. El-Sharkawi, Optimal charging strategies for unidirectional vehicle-to-grid, IEEE Trans. on Smart Grid 2 (2011) 119-126.

[9] N. Rotering, M. Ilic, Optimal charge control of plug-in hybrid electric vehicles in deregulated electricity markets, IEEE Trans. on Power Sys. 26 (2011) 1021-1029.

[10] R.J. Bessa, M.A. Matos, Global against divided optimization for the participation of an EV aggregator in the day-ahead electricity market – Part I: theory, submitted to Elec. Power Sys. Res. (2012).

[11] F.J. Soares, J.A. Peças Lopes, P.M.R. Almeida, C.L. Moreira, L. Seca, A stochastic model to simulate electric vehicles motion and quantify the energy required from the grid, Proc. of the 17th PSCC Conf. (2011), Stockholm, Sweden.

[12] INE - Instituto Nacional de Estatística, Inquérito à mobilidade da população residente. Questionnaire about the Portuguese population mobility, (2000) (in Portuguese).

[13] F.J. Soares, Impact of the deployment of electric vehicles in grid operation and expansion, PhD Thesis, University of Porto - FEUP (2012).

[14] S. Bending, S. Channon, M. Ferdowsi, K. Strunz, E. Bower, A. Walsh, et al., Specification for an enabling smart technology, Deliverable D1.1 European Project MERGE (2010). [Online] http://www.ev-merge.eu

[15] E.L. Miguélez, I.E. Cortés, L. Rouco, G. López, An overview of ancillary services in Spain, Elec. Power Sys. Res. 78 (2008) 515-523.

[16] P. Pinson, C. Chevallier, G. Kariniotakis, Trading wind generation with short-term probabilistic forecasts of wind power, IEEE Trans. on Power Sys. 22 (2007) 1148-1156.

[17] e·sios (Red Eléctrica de España, REE) April 2012. [Online] http://www.esios.ree.es/web-publica/

[18] REN market data April 2012. [Online] http://www.mercado.ren.pt/Paginas/default.aspx

[19] OMIE (Market Operator of MIBEL) April 2012. [Online] http://www.omie.es/inicio

[20] P.E. Morthorst, S. Wagemans, K. Purchala, A. Woyte, A. Ceña, A. Mora, et al., Detailed investigation of electricity market rules - Cases for France, Germany, Netherlands, Spain and Denmark, Deliverable 4.1 European Project TradeWind (2007). [Online] http://www.trade-wind.eu

[21] A. Botterud, Z. Zhou, J. Wang, R.J. Bessa, H. Keko, J. Sumaili, V. Miranda, Wind power trading under uncertainty in LMP markets, IEEE Trans. on Power Sys. 27 (2012) 894-903.

[22] R. Herranz, A.M. San Roque, J. Villar, F.A. Campos, Optimal demand-side bidding strategies in electricity spot markets, IEEE Trans. on Power Sys. In Press (2012). DOI: 10.1109/TPWRS.2012.2185960

[23] M. Herrera, L. Torgo, J. Izquierdo, R. Pérez-García, Predictive models for forecasting hourly urban water demand, J. of Hydro. 387 (2010) 141-150.

[24] D. Kwiatkowski, P.C.B. Phillips, P. Schmidt, Y. Shin, Testing the null hypothesis of stationarity against the alternative of a unit root, J. of Econometrics 54 (1992) 159-178.

[25] A. Hirotugu, A new look at the statistical model identification, IEEE Trans. on Auto. Cont. 19 (1974) 716-723.

[26] M. Gilliland, Is forecasting a waste of time?, Suppl. Chain Manag. Rev. 6 (2002) 16-23.

[27] M. Sokolova, G. Lapalme, A systematic analysis of performance measures for classification tasks, Info. Proc. and Manag. 45 (2009) 427-437.

[28] J. Pinheiro, D. Bates, S. DebRoy, D. Sarkar, R Development Core Team. nlme: Linear and Nonlinear Mixed Effects Models, (2011) R package version 3.1-102.

[29] S.N. Wood, Generalized Additive Models: an Introduction with R, Chapman and Hall/CRC, London, 2006.

[30] A. Gelman, Y. Su, M. Yajima, J. Hill, M.G. Pittau, J. Kerman, T. Zheng, arm: Data analysis using regression and multilevel/hierarchical models, (2011) R package version 1.4-13. [Online] http://CRAN.R-project.org/package=arm

[31] IBM ILOG CPLEX V12.2: User's Manual for CPLEX International Business Machines Corporation, 2010.

[32] A.R. Hatami, H. Seifi, M.K. Sheikh-El-Eslami, Optimal selling price and energy procurement strategies for a retailer in an electricity market, Elec. Power Sys. Res. 79 (2009) 246-254.

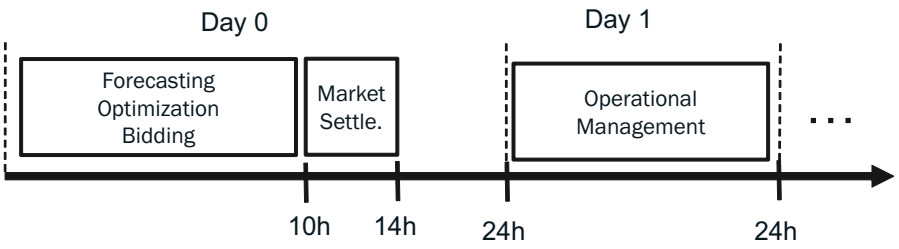

Figure 1: Diagram with the sequence of tasks for participating in the Iberian electricity market.

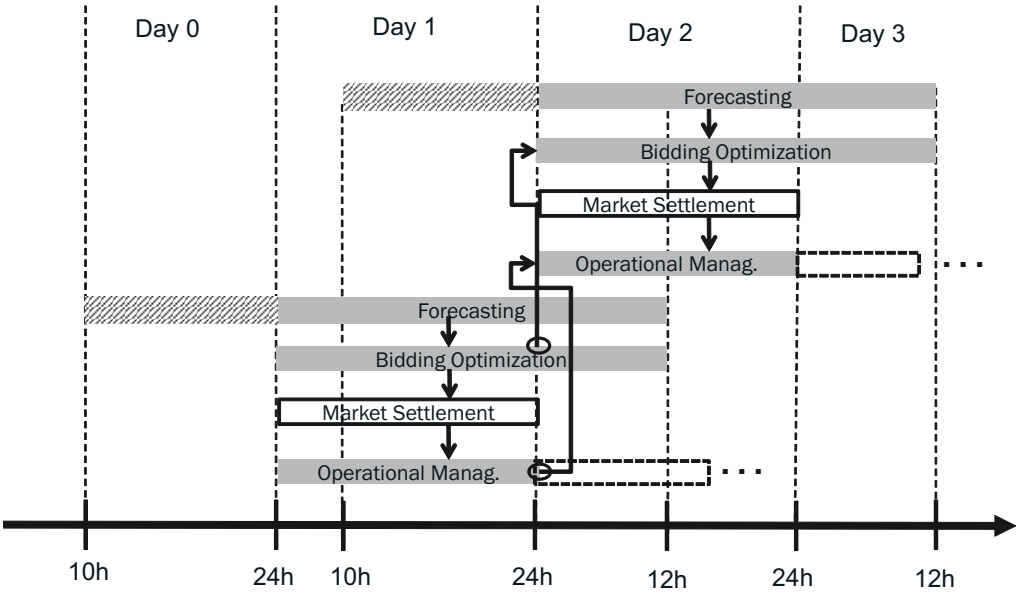

Figure 2: Diagram with the temporal horizons of the forecast and optimization algorithms.

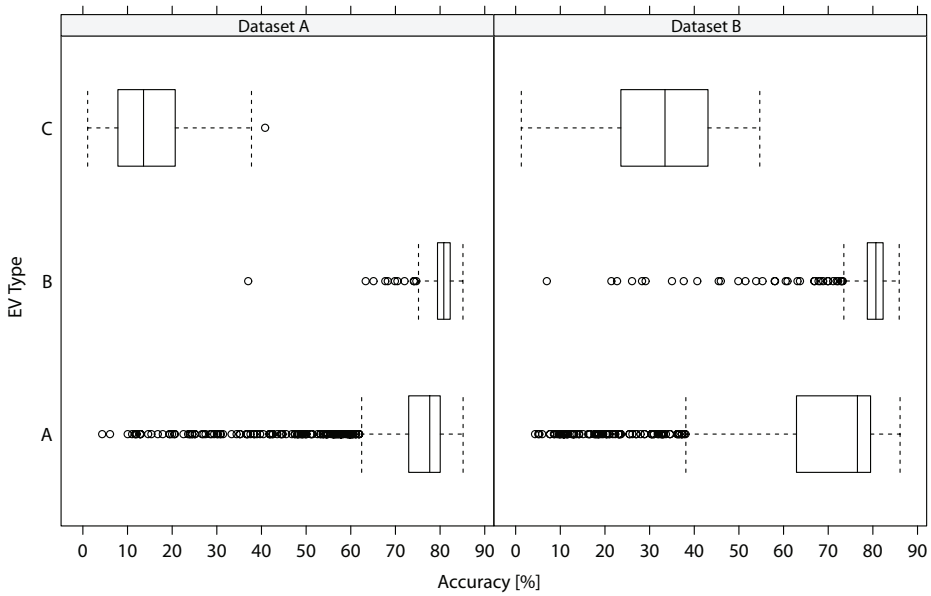

Figure 3: Boxplot for the accuracy of the availability forecast and for dataset A and B. The boxplot have five statistics: lowest datum (within 1.5 IQR) of the lower quartile, lower quartile, median, upper quartile, and the highest datum (within 1.5 IQR) of the upper quartile. The outliers are also identified on the boxplot.

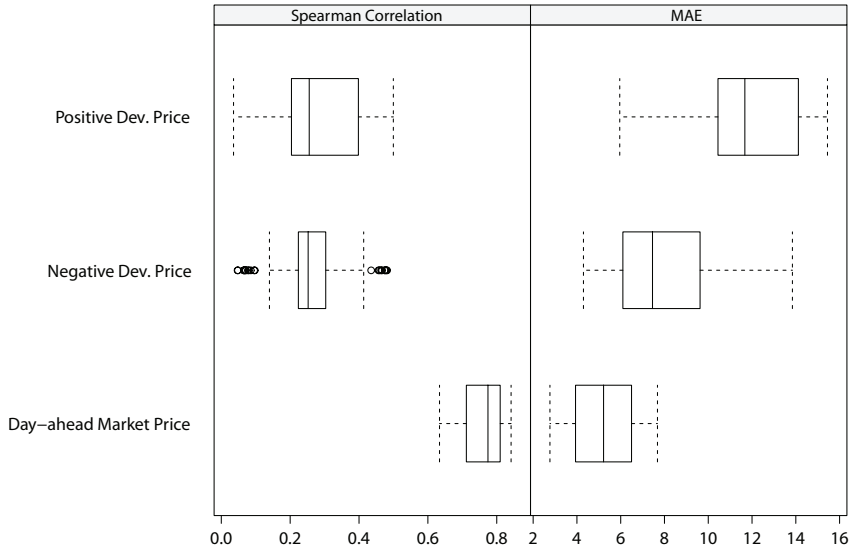

Figure 4: Spearman correlation and mean absolute error of the prices forecasts for 100 samples.

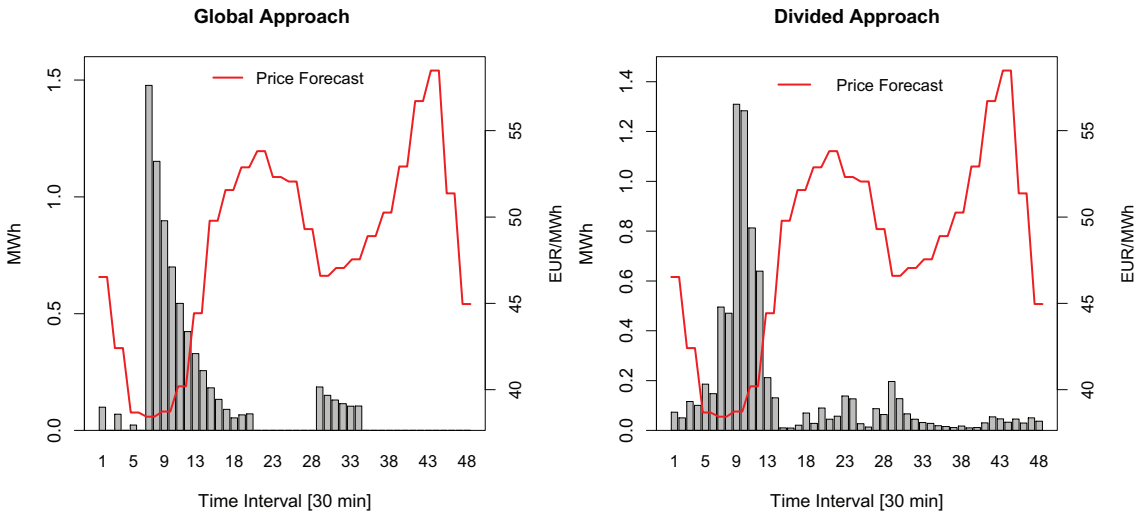

Figure 5: Optimized bids obtained from the divided and global approaches for day 6 of the test period.

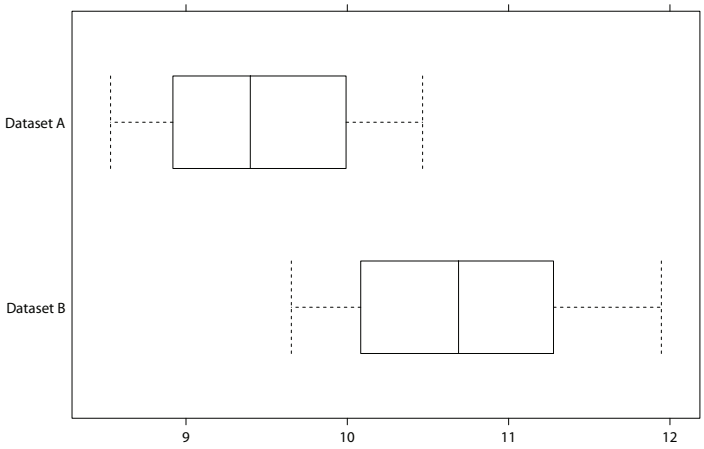

Figure 6: mMAPE of the divided approach with forecasted information for dataset A and B.

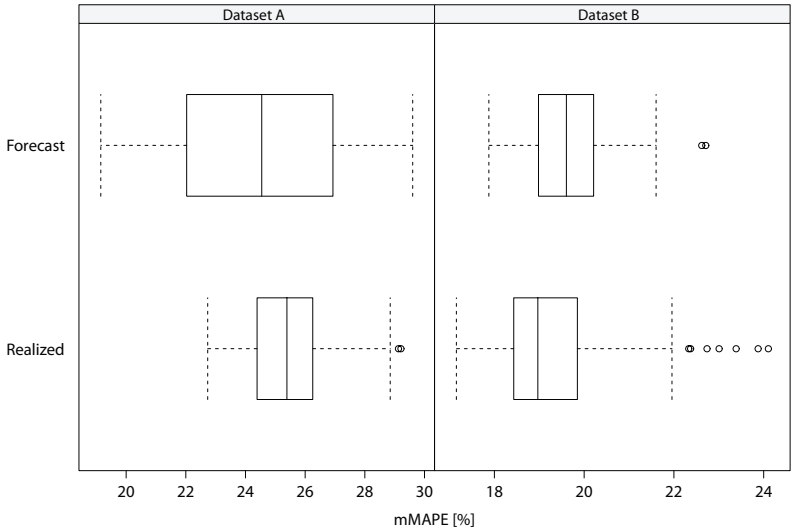

Figure 7: mMAPE of the global approach with forecasted and realized information for dataset A and B.

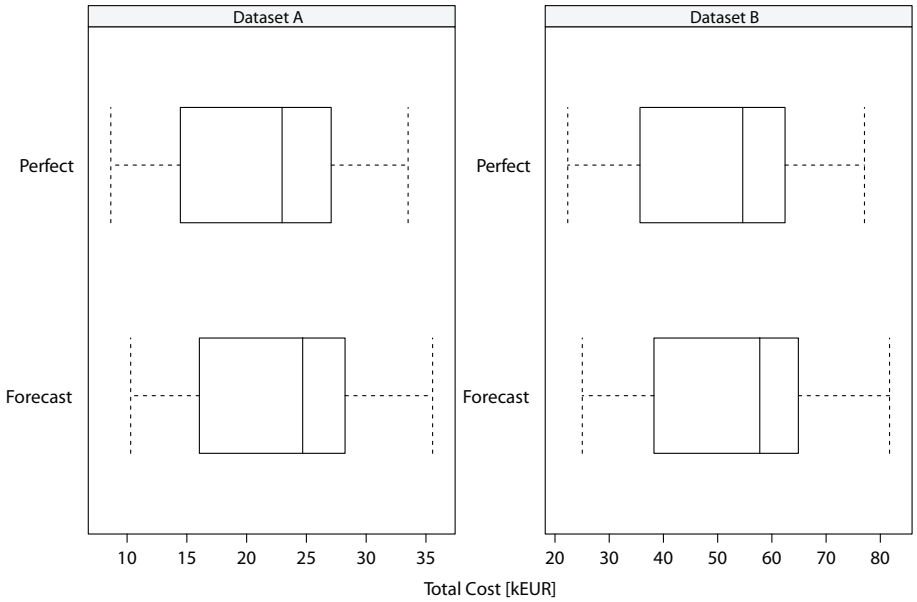

Figure 8: Results with perfect and forecasted information for the divided approach in dataset A and B.

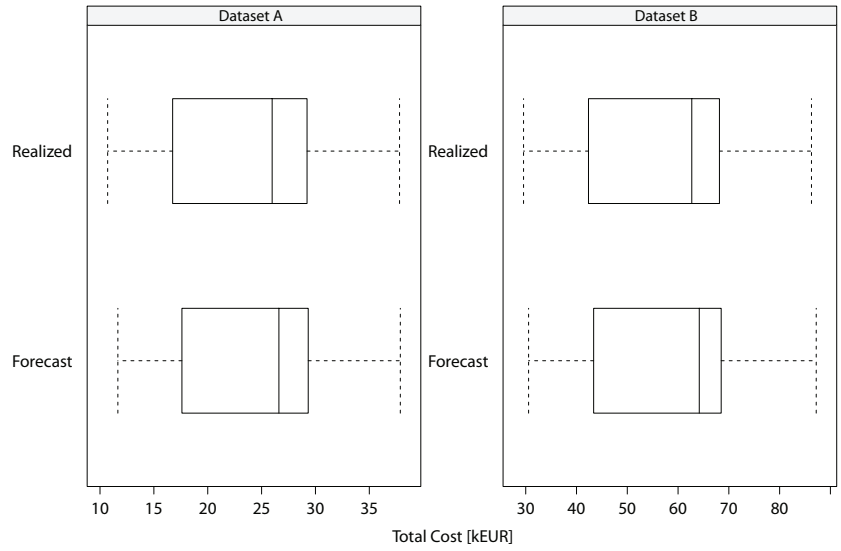

Figure 9: Results with perfect and forecasted information for the global approach in dataset A and B.

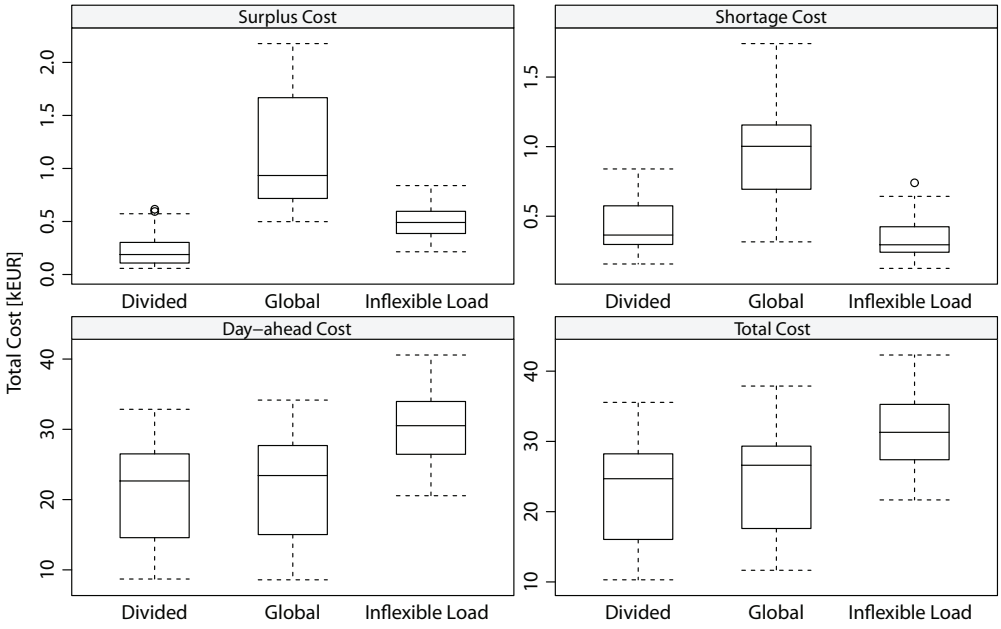

Figure 10: Costs comparison between divided, global and inflexible EV load approaches obtained using forecasted values for dataset A.

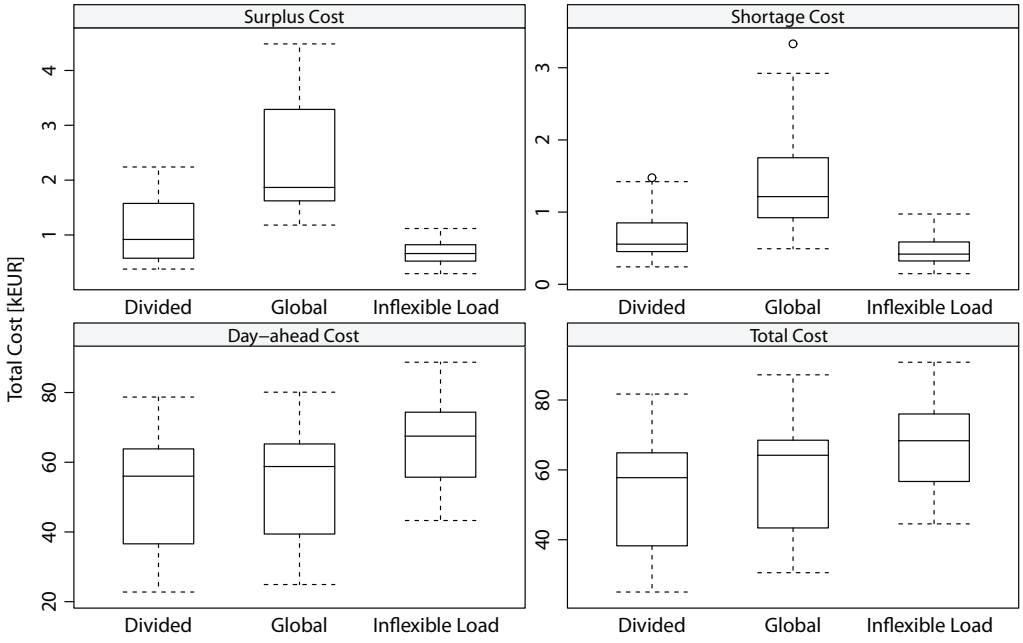

Figure 11: Costs comparison between divided, global and inflexible EV load approaches obtained using forecasted values for dataset B.

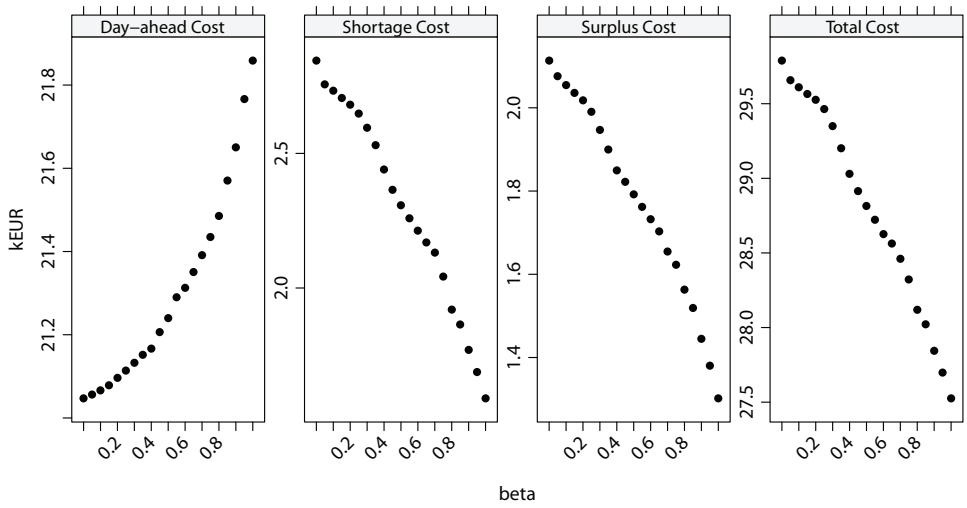

Figure 12: The impact of β in the total cost shares for dataset A with 1500 EV.

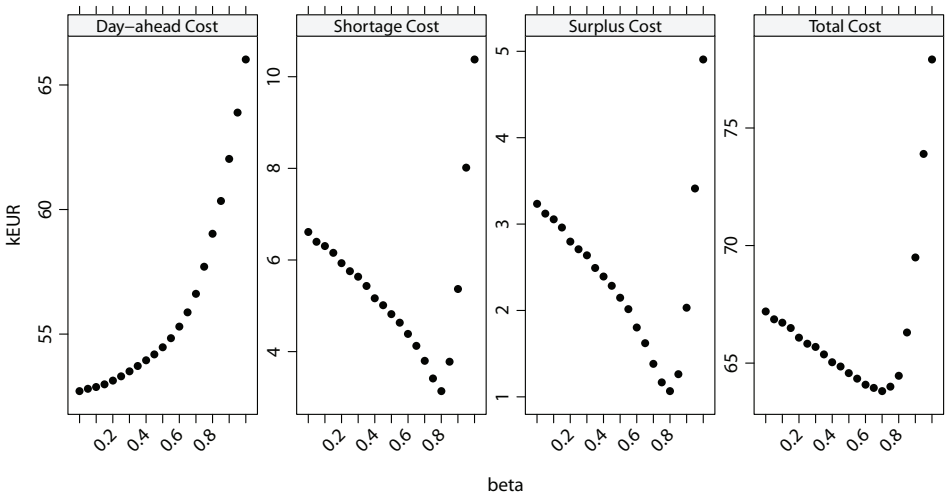

Figure 13: The impact of β in the total cost shares for dataset B with 1500 EV.

Table 1: Three types of behavior regarding EV charging.

Type	Behavior	Percentage of the Responses
A	EV charge at the end of the day	57%
B	EV charge whenever possible	20%
C	EV charge only when it needs	23%

Table 2: Forecasting performance for the EV aggregated variables for dataset A and B.

	Dataset A		Dataset B	
	MAPE [%]	PBIAS [%]	MAPE [%]	PBIAS [%]
Maximum available power for charging [MW]	5.46	-0.62	5.31	-0.76
Total charging requirements [MWh]	19.43	0.17	17.12	-0.24
Total charging requirements distribution [MWh]	8.99	-1.89	7.53	-1.51
Total Inflexible Load [MWh]	15.75	-3.01	9.60	-1.54

Table 3: Retailing tariff value that leads to a breakeven between total cost and retailing revenue.

	Divided	**Global**	**Inflexible Load**
Dataset A	0.033 kWh	0.036 kWh	0.045 kWh
Dataset B	0.035 kWh	0.038 kWh	0.042 kWh